


Model-based full reference image blurriness assessment

Mohammad Hossein Khosravi¹  · Hamid Hassanpour¹

Received: 8 June 2015 / Revised: 20 October 2015 / Accepted: 7 December 2015 /
Published online: 21 January 2016
© Springer Science+Business Media New York 2016

Abstract Measuring image blurriness is an important issue in image-quality assessment. The blurriness affects the image quality by degrading the image's high frequency details in the form of some uniform redundancies in neighboring pixels. Indeed, the blurriness is accompanied with two distortions: corrupted high frequency details, and degraded image structure due to the redundancies. In this paper, we propose an approach that measures the effects of these two distortions using singular value decomposition (SVD). From the properties of SVD, the basis images corresponding to the higher singular values are associated with the structural information of the image, while the ones corresponding to the lower singular values are related to the image details. This work employs this property and splits the ordered singular values into two subsets from a non-fixed separation point, and constructs two images by stacking up the basis images corresponding to these two subsets. By moving the separation point for these two subsets and computing the energy of the two constructed images in each point, two sequences of energies will be in hand. We show that the behavior of these two sequences can be used to assess the amount of both structural distortions and nonstructural detail degradations of an image, and hence a valuable blur metric. Experimental results illustrate that there is a well correlation between the results of our blur metric and human scores. In addition, in comparative experiments, we found that the proposed blur metric stands among the best state-of-the-art ones in evaluating quality of images in terms of blurriness.

Keywords Image blurriness evaluation · Structural information · Low frequency redundancies · Singular value decomposition

✉ Mohammad Hossein Khosravi
mohokhosravi@shahroodut.ac.ir

¹ Laboratory of Image Processing and Data Mining, University of Shahrood, Shahrood, Iran

1 Introduction

Assessing the quality of an image is one of the most important and indispensable issue in image processing. The best reference for evaluating the quality of an image might be human being. However it might be person-dependent, expensive, time-consuming and tedious, especially when applied to a huge number of images.

Objective metrics, on the other hand, provide a quantitative measure in an acceptable time and with a reasonable precision. These metrics can be classified in three categories, namely, full-reference (FR), reduced-reference (RR) and no-reference (NR) metrics, based on their need to the reference image information. Full-reference objective metrics need the pristine reference image to compare with the image under evaluation. These metrics have a crucial role in tuning image processing systems that their process accompanied with some degradations. Image compression is an example of such systems. The reduced-reference methods need only some descriptive information about the reference image. These metrics are often used in transmission issues where the quality of received images are assessed with extra information. The no-reference methods evaluate the quality of an image without the need for the reference image. These methods are difficult to develop because they need intrinsic information about the quality of the image.

An image might be affected by various distortions, which can be categorized in non-structural and structural ones [25]. Nonstructural distortions, like a change of luminance or brightness, a change of contrast, Gamma distortion, and spatial shifts, impose unpleasant visual effects on image without destroying its structure; while the structural distortions, like additive noise, blurring and lossy compression, ruin the major structure of image so that the observer cannot distinguish the image contents in severe conditions. Blurriness, among these distortions, is a common structural distortion, which has been assessed in various ways, that can be categorized in spatial and non-spatial methods. The spatial methods, often, model the total or local variations on statistics like variance [5, 21], autocorrelation and energy of the first and second derivatives [2], edge profile distributions [1, 4, 6], or dominant eigenvalues of image covariance matrix [28], and use them to define a metric to assess the blurriness. These methods have the benefits of low complexity cost. The non-spatial methods obtain their features through some suitable subband or statistical decompositions. These methods often describe images through varieties of basis functions and then attempt to assess the blurriness by estimating the amount of energy attenuation in the high frequency basis functions. In [3] blurriness is measured as the kurtosis of DCT coefficients of blocks. In [11] the uniformity of image spectrum is assessed by entropy and is used as a blurriness metric. Another blur metric called FISH [22], uses the logarithm of wavelet sub-band energies in three different scales. In [9, 10] the local phase coherence in wavelet domain is measured and is employed in computing the blurriness metric. The authors in [20] performed an SVD decomposition on image and employed the ratio between the k most significant singular value and all singular values as a blur metric. In [16] the properties of singular values curve is used to assess the blurriness.

In this paper we evaluate the blurriness of an image by considering both its structural and nonstructural residual defections. Proposed blur metric employs the structural and residual features arises from the SVD-based basis images, which formed from the product of the left and right singular vectors, accompanied with the corresponding singular value. In recent years, there has been an increasing attention to SVD as an efficient decomposition for image quality assessment. For instance, beside two aforementioned SVD-based blur metrics in [16, 20], there exist methods like those proposed in [19, 23, 24, 31], which their main concern are overall quality evaluation, but their results on blurriness are also noticeable.

The rest of this paper is organized as follows: Sections 2.1 and 2.2 give a brief review on the singular value decomposition concepts and the basis images analysis, respectively. A detailed description of our proposed measure is given in Section 2.3. Performance evaluations and results analysis are presented in Section 3. Finally the paper is concluded in Section 4.

2 Proposed SVD-based blur evaluation metric

2.1 A brief review of singular value decomposition

The singular value decomposition is one of the most efficient tools in linear algebra to decompose a matrix into a series of basis matrices which represent the underlying structure of the matrix. Every real matrix X with dimension $m \times n$ can be decomposed into a three matrices as below,

$$X = U_{m \times r} \times S_{r \times r} \times V_{r \times n} \tag{1}$$

where U and V are orthogonal matrices ($U^T U = I, V^T V = I$) containing left and right singular vectors of X , respectively, and S is a diagonal matrix containing the singular values of X in descending order. The number of non-zero singular values, r , is the rank of matrix X . These matrices can be shown as below,

$$\begin{cases} U = (u_1, u_2, \dots, u_r) \\ V = (v_1, v_2, \dots, v_r) \\ S = \text{diag}(\delta_1, \delta_2, \dots, \delta_r) \end{cases} \tag{2}$$

Considering the above, (1) can be rewritten as below:

$$X = \sum_{i=1}^r X_i = \sum_{i=1}^r u_i \delta_i v_i^T \tag{3}$$

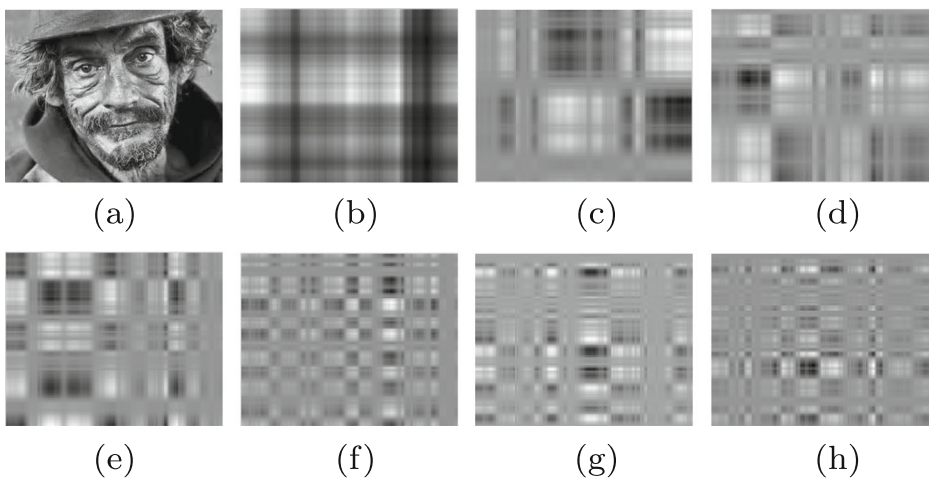


Fig. 1 (a) Original Image, (b-h) Basis images corresponding to the seven higher singular values of image (a), respectively

The basis images (X_i) corresponding to higher singular values contain the major information of image which encoded in its low frequency components. On the other hand the ones corresponding to lower singular values expose the nonstructural details of the image, i.e. the high frequency contents. Figure 1b-h show the basis images corresponding to the seven higher singular values of the reference image shown in Fig. 1a. The number of basis images which can be extracted for an image is equal to the rank of the image, $r \leq \min(\text{rows}, \text{columns})$.

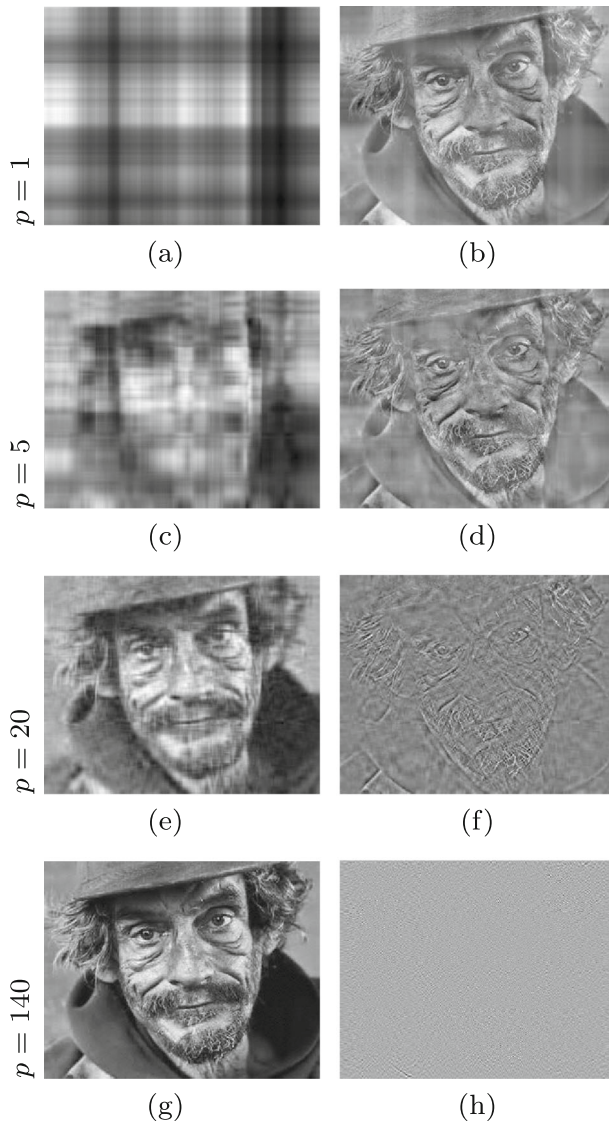


Fig. 2 Illustration of the structural (*left*) and residual (*right*) portions of the reference image shown in Fig. 1(a), for the various values of $p \in \{1, 5, 20, 140\}$. Note the pixel intensities is scaled to $[0,255]$ for better representation

2.2 Structural and residual portions of an image

Recall (3), by setting a positive integer p , $0 \leq p \leq r$ and computing the summations in (4), we can obtain two complementary portions of image X , which we call them Structural Portion (SP) and nonstructural Residual Portion (RP).

$$\begin{cases} SP_X^p = \sum_{i=1}^p u_i \delta_i v_i^T \\ RP_X^p = \sum_{i=p+1}^r u_i \delta_i v_i^T \end{cases} \tag{4}$$

For small values of p , the SP portion contains the major structure of the image without its high frequency components, while these high frequency components will be in RP portion. By increasing the value of p toward r , the SP portion will become more similar to the original image and the RP portion will become sparser. Figure 2 shows the two portions SP and RP for different values of p .

The concepts of structural and residual portions have been introduced in [23] (namely, content-dependent and content-independent parts), where they employed the gradient and contrast similarities between the content-dependent parts of the reference and the distorted images, besides the normalized PSNR of content-independent parts. Here we concentrate on the inherent properties of these portions and obtain more accurate results for assessing blur.

Back to (4), the energy of structural and residual portions (ESP_X and ERP_X , respectively), for a given value of p , can be calculated via Frobenious norm as below¹,

$$\begin{cases} ESP_X^p = \|SP_X^p\|_F = \sqrt{\sum_{i=1}^p \delta_i^2} \\ ERP_X^p = \|RP_X^p\|_F = \sqrt{\sum_{i=p+1}^r \delta_i^2} \end{cases} \tag{5}$$

The resulted vectors contain valuable information about the image blurriness. To further investigate, let we choose an arbitrary source image and produce various of its blurred version via applying Gaussian smoothing filters with different values of σ . The ESP_X and ERP_X of the image for various p have been computed and shown in Fig. 3. As it can be considered from the figure, the slope of changes in ESP_X and ERP_X highly depends to the image blurriness. These behaviors, from our experience on various reference images, can be described mathematically as below:

$$\begin{cases} ESP_X^p \approx \log(p^\alpha) \\ ERP_X^p \approx \frac{1}{\log(p^\beta)} \end{cases} \tag{6}$$

where the values of α and β determine the curves in Fig. 3a and b, respectively, and are proportional with the variance (σ) of the Gaussian function involved in blurriness.

2.3 Proposed method of blurriness assessment

The blurriness affects the image quality by decreasing the image’s high frequency details and introducing to the low frequency components in the form of some uniform redundancies in neighboring pixels. Hence, we face with two kinds of destructions, first losing the high frequency details, and second damaging the image structure by introducing the low frequency redundancies. Here, we try to estimate both of these effects by considering the properties of ESP_X^p and ERP_X^p , respectively. To do this, the sequences ESP_X^p and ERP_X^p

¹From linear algebra, it is known that: $\|USV^T\|_F = \sqrt{\text{Tr}[(USV^T)(USV^T)^T]} = \sqrt{\text{Tr}(USV^T V S^T U^T)} = \sqrt{\text{Tr}(SS^T)}$

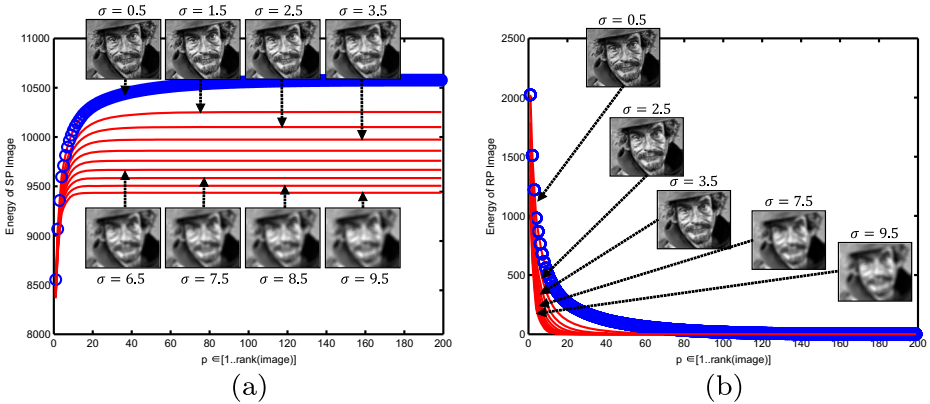


Fig. 3 Plots of vectors (a) ESP_X and (b) ERP_X , corresponding to the energy of structural and residual portions, respectively, for the blurred versions of image in Fig.1(a), with variances $\sigma \in [0.5, \dots, 9.5]$ with steps of 1. The circle symbols indicate the corresponding energies of the reference image

are computed for both the reference and the blurred images, and then the following ratios are built upon them:

$$\frac{ESP_B^p}{ESP_R^p} \approx \frac{\log(p^{\alpha_B})}{\log(p^{\alpha_R})} = \frac{\alpha_B \log(p)}{\alpha_R \log(p)} = \frac{\alpha_B}{\alpha_R} \tag{7}$$

$$\frac{ERP_B^p}{ERP_R^p} \approx \frac{\frac{1}{\log(p^{\beta_B})}}{\frac{1}{\log(p^{\beta_R})}} = \frac{\beta_R \log(p)}{\beta_B \log(p)} = \frac{\beta_R}{\beta_B} \tag{8}$$

where α_R and β_R determine the curves of structural and residual portion energies, respectively, belong to the reference image. Similarly, the values of α_B and β_B indicate the corresponding curves in blurred image. Since the values of α_R and β_R are constant for a given reference image, the ratios in (7) and (8) can determine the rate of blurriness. These ratios characterize the structural and residual distortions, respectively, and can be served in a blur indicator. We involve their contribution via a nonlinear pooling scheme and make our final proposed Blur Metric (BM), as below:

$$proposed\ BM = \frac{1}{q} \left(\sum_{p=1}^q \frac{ESP_B^p}{ESP_R^p + \epsilon} \right)^\gamma \cdot \left(\sum_{p=1}^q \frac{ERP_B^p}{ERP_R^p + \epsilon} \right)^{1-\gamma} \tag{9}$$

where the parameter γ , $0 \leq \gamma \leq 1$, is a tuning parameter and can be determined empirically to achieve the best correlation with the subjective scores. In the next section we will provide more discussion around this parameter. In order to avoid division by zero, the extra small value of ϵ is added in the denominators. The dynamic range of our proposed blur metric is (0, 1], with the best value achieved when the blurred and the reference images are equal. Figure 4 exhibits a flowchart for the proposed full-reference blur evaluation algorithm.

3 Performance evaluation

In the implementation stage, we must determine two parameters in our proposed method. First the parameter q in (5), which determines the size of sequences SP_R^p and RP_R^p , and is a

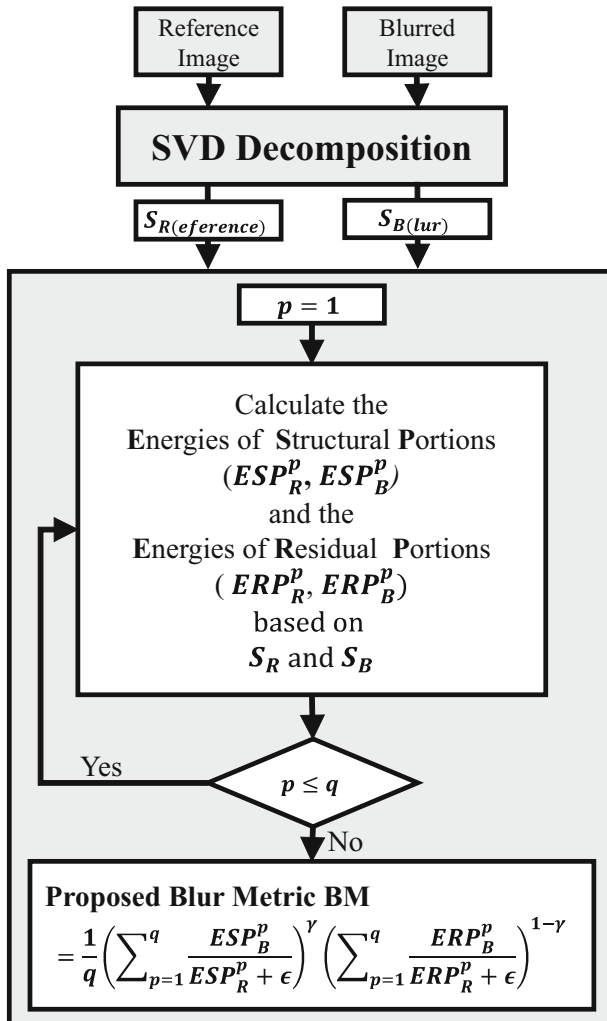


Fig. 4 Flowchart of the proposed SVD-based image blur assessment approach

nonzero value smaller than the rank of the image. We found empirically that the best value of this parameter is around $q = \lfloor \frac{\min(m,n)}{3} \rfloor$. The second parameter to set, is the value of γ in (9) which controls the contribution of the two aforementioned portions. Through a series of experiments, which will be explained in the following subsection, this parameter sets as $\gamma = 0.95$.

A popular method for validating the ability of a blur metric is to investigate the algorithm’s performance in monotonically predicting the blurriness of images with uniformly increasing the standard deviation. In the first experiment, we have produced several blurred images with different standard deviation $\sigma \in \{0.5, 1.5, \dots, 9.5\}$. Figure 5 shows the values of the proposed blur metric for these blurred images against the values of standard deviation. As the figure shows, by increasing the blurriness, the values of the proposed metric are decreased monotonically.

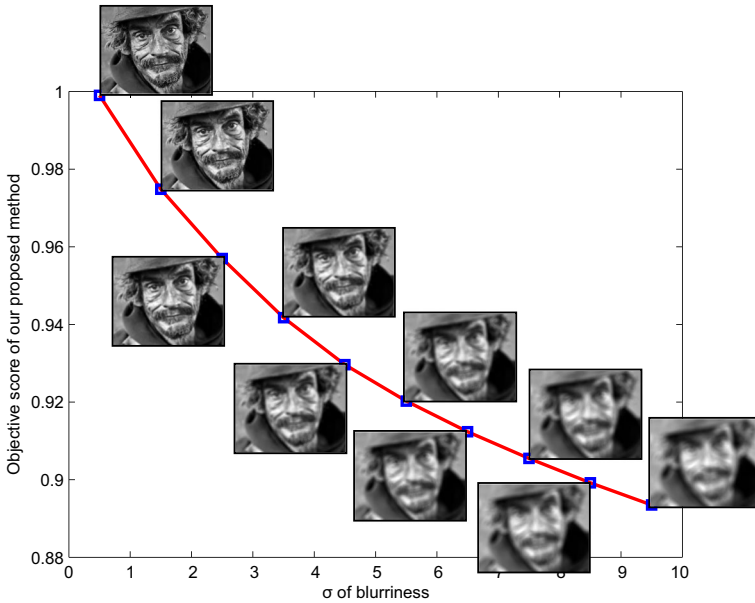


Fig. 5 The plot of objective scores of blurriness, evaluated by proposed blur metric, versus different variance (σ) values in blurring the image

In order to further evaluate the proposed blur metric, we verify its ability to predict the subjective scores of the blurred image subsets of LIVE(Laboratory for Image and Video Engineering) [18], TID2008 [15] and CSIQ [12] databases. The LIVE is a standard database for image quality metrics performance evaluation, which contains 29 high-resolution original and 145 Gaussian blurred images. The TID2008 is a comprehensive quality-related database with 25 reference images blurred each in four levels of blurriness. The CSIQ is also a popular quality related image database, contains 150 blurred images (30 references each blurred in five different severity).

We used four criteria to assess the performance of proposed algorithm following [8]: (1) The Pearson correlation coefficient (PCC), which measures the amount of predictions correlation with the subjective scores, (2) The Spearman rank order correlation (SROCC) and (3) the Kendall rank order correlation (KROCC), which measure both the relative monotonicity between the predictions and subjective scores, and (4) the root mean square error (RMSE) which validates the predictions accuracy, like PCC. Before evaluating these criteria, we applied the following five-parameter logistic transform suggested by [8], to the values obtained from our blur metric to bring them on the same scales as the TID2008’s MOS, LIVE’s DMOS and CSIQ’s DMOS values:

$$MOS_e = \beta_1 \left(\frac{1}{2} - \frac{1}{1 + \exp(\beta_2 BM - \beta_3)} \right) + \beta_4 BM + \beta_5 \tag{10}$$

where MOS_e is the estimated MOS by our proposed blurriness metric BM . The coefficients β_i are determined so that the minimum MSE between the MOS and the MOS_e achieved. Figures 6a, c and e show the scatter plots of the objective scores for the proposed blur metric versus the subjective ones of TID2008, LIVE and CSIQ databases, respectively. The solid curves are the results fitted with the above logistic function. In addition, the scatter plots of

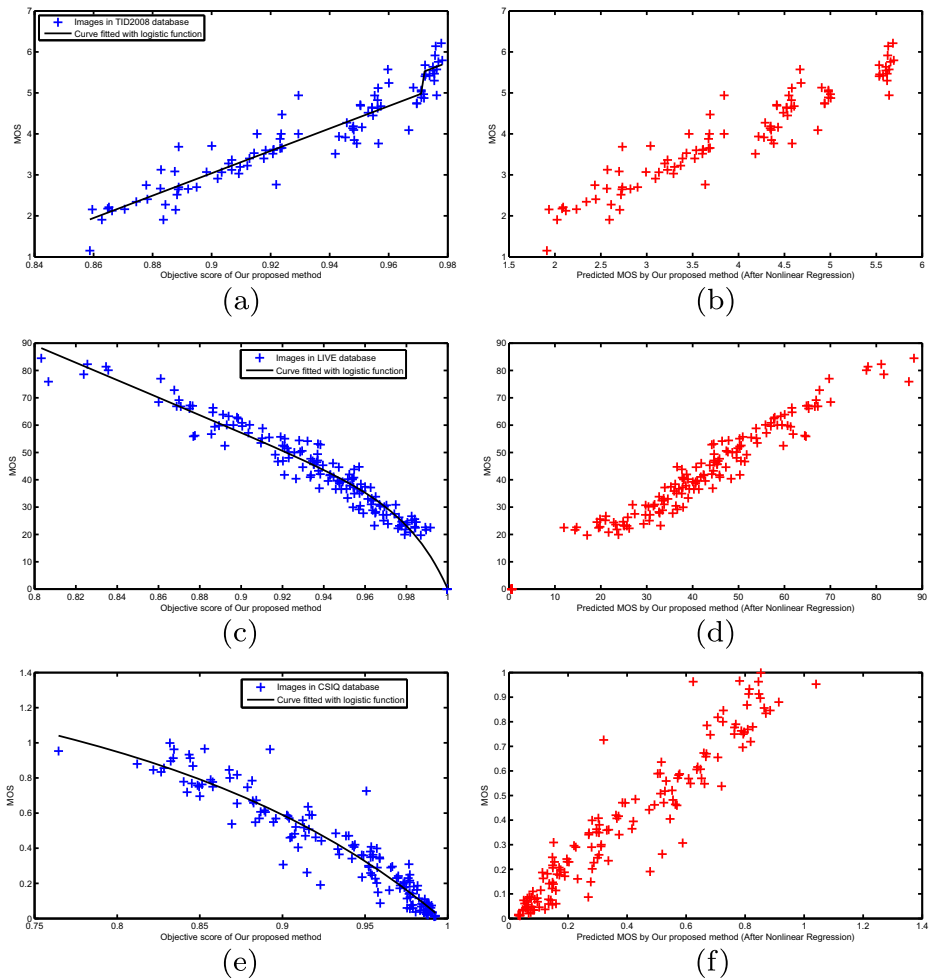


Fig. 6 Scatter plots of subjective scores versus the proposed blur metric on blurred subsets of IQA databases: (a) TID2008, (c) LIVE and (e) CSIQ databases. (b), (d) and (f) Scatter plots of the same data as (a), (c) and (e), respectively, after nonlinear regression. The corresponding evaluation criteria are shown in Table 1

MOS_e versus MOS is shown in Fig. 6b, d and f, for TID2008, LIVE and CSIQ databases, respectively. The correlation between the values of MOS_e and MOS demonstrates that the proposed metric has well consistency with human opinions of quality. In addition Table 1 shows the values of the predefined evaluation criteria for the proposed blur metric on these databases. It can be observed that the PCC and SROCC between the scores of the proposed metric and the subjective scores of test databases are impressive.

Table 1 The values of performance evaluation criteria for the proposed blurriness metric

	PCC	SROCC	KROCC	RMSE
LIVE	0.9845	0.9788	0.8780	3.8179
TID2008	0.9485	0.9543	0.8241	0.3674
CSIQ	0.9525	0.9570	0.8229	0.0873

Table 2 the values of SROCCs of some blurriness metrics applied on subset of blurred images of LIVE, TID2008 and CSIQ databases

	Proposed	PSNR	SSIM	MS-SSIM	ADM	VIF	MAD	FSIM	SVDR	VGS	ref[24]
LIVE	0.9788	0.9413	0.9517	0.9722	0.9650	0.9584	0.8990	0.9708	0.9123	0.9700	0.9775
TID2008	0.9543	0.8682	0.9544	0.9607	0.9140	0.9546	0.9197	0.9472	0.8120	0.9040	0.9696
CSIQ	0.9570	0.9289	0.9609	0.9720	0.9726	0.9747	0.9660	0.9729	0.9367	0.9820	0.9839

As another validation step, we compare the results of the proposed method with the results of some other well accepted quality metrics including PSNR, SSIM [27], MS-SIM [26], ADM [13], VIF [17], MAD [12], FSIM [29], SVDR [14], VGS [30] and the SVD-ELM based method proposed in [24]. In this comparison, we only employ the SROCC criterion and forget the others because of their similar results. As Table 2 shows, the SROCC of the proposed method on LIVE database dominates the SROCC of all other metrics, which is an impressive achievement. For TID2008 and CSIQ databases, our proposed metric doesn't sit among the three dominant metrics, but its distances to them are not considerable.

3.1 The role of Gamma

Recall from (9), our proposed blur metric is achieved through an exponentially weighted pooling scheme, in which the parameter γ controls the amount of contributions of structural and residual portions. A series of experiments performed on TID2008, LIVE and CSIQ databases with the aim of detecting the best value of this parameter. Figure 7 indicates the resulted SROCC between the MOS values of these image databases and the objective

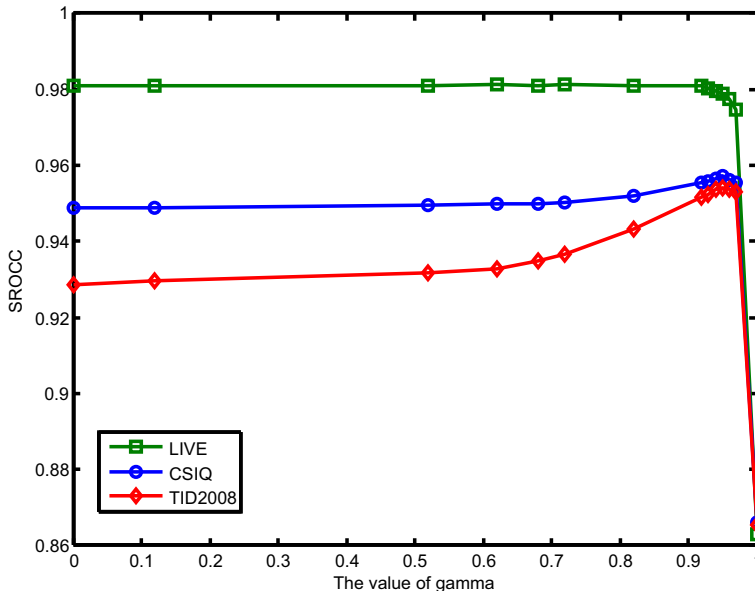


Fig. 7 The plot of different SROCC values between the MOS provided by TID2008, LIVE and CSIQ image databases and proposed blur metric scores, versus different values of γ in (9)

blur measures achieved by our blur metric with different values of $\gamma \in [0, 1]$. Surprisingly eliminating the second term in (9) (i.e. the rate of residual portion energies) by setting the value of $\gamma = 1$, exposes more destructive effect on blur metric, compared to removing the first term (i.e. the rate of structural portion energies) by setting $\gamma = 0$. It can be realized that the existence of residual portion information, has impressive improvement on the proposed metric, even with an small exponential weight. The reason was investigated by observing the behavior of the first and the second terms in (9), separately, for different blur versions of the first image of TID2008 database, namely "I01.bmp", which are shown in Fig. 8. As can be seen in Fig. 9, the first term in (9) has a low sensitivity to the blur severity, while the second term behaves in opposite direction and expresses a high keenness to the blurriness extremity. These different dynamic ranges of changes for these two terms were foresighted. The first term always includes the first singular value of the image, which is the most dominant

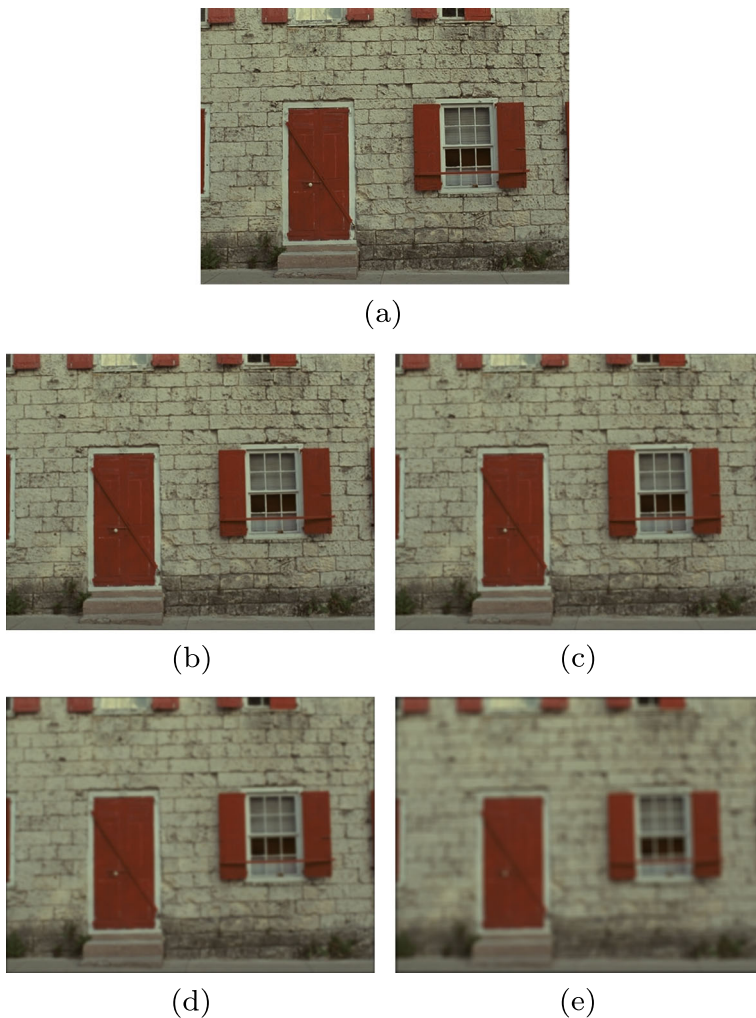


Fig. 8 The first image of the TID2008 database (i.e. 'I01.bmp'). **a** the original image, **(b-e)** four blurred versions of **(a)** with increasing blur severity

one. On the other hand the second term includes the details information, which changes drastically by introducing blur effects. These observations reinforce our assumption about the two kinds of destructions in a blurred image.

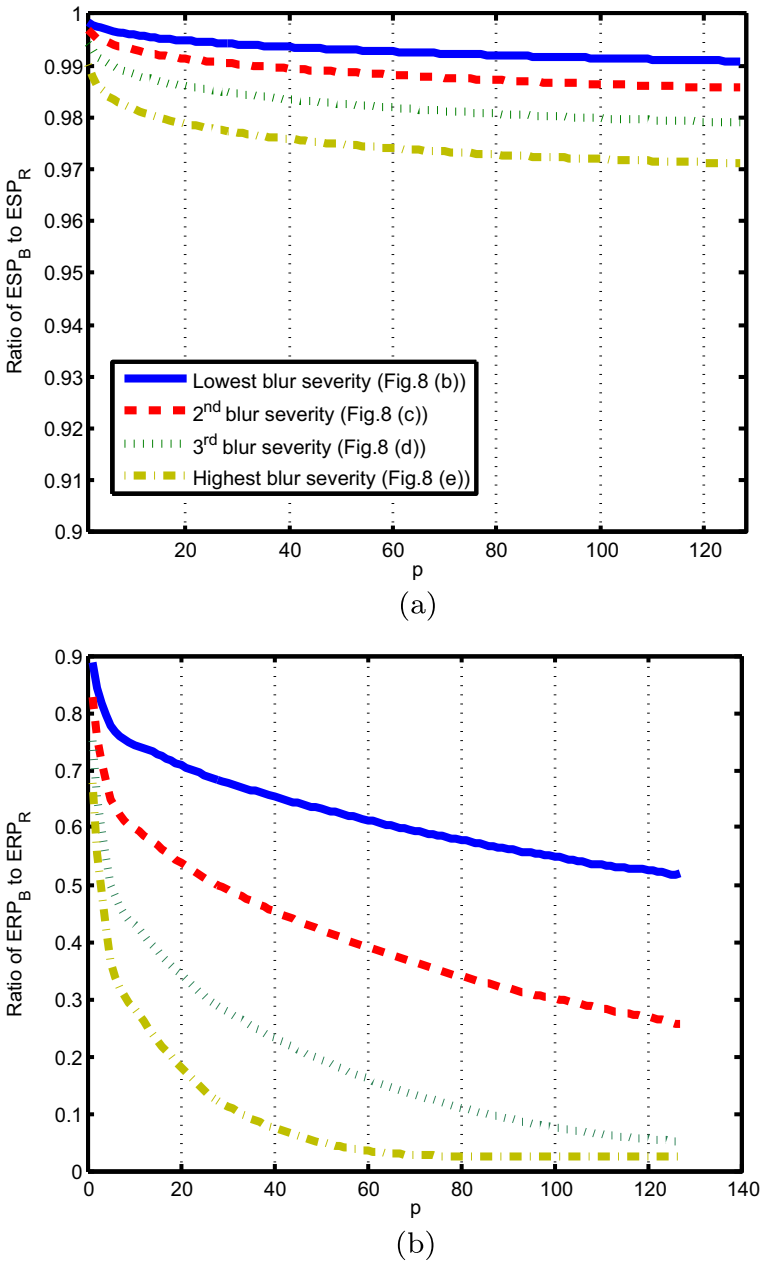


Fig. 9 The different dynamic ranges of (a) the first term, and (b) the second term of (9), before exponentially weighting by γ , for different blurred versions of the first image of the TID2008’s image database, shown in the Fig. 8(b-e). Please note to the scale of vertical axis in the both two plots

Table 3 Consuming time for each IQA index (in seconds per image)

	PSNR	SSIM	MS-SSIM	Proposed	ADM	VSI	FSIM	VIF	MAD	IFC
TID2008	0.0177	0.0523	0.0789	0.1086	0.1361	0.3244	0.3621	1.1960	1.3768	2.5967

Back to Fig. 7, the value of $\gamma = 0.82$ is the best when we consider only the LIVE database. This setting yields an SROCC equal to 0.9812 for this database, which is a very good score. But to have a reasonable results on the whole three aforementioned databases, we set the final value of this parameter as $\gamma = 0.95$.

3.2 Computational complexity of proposed metric

In order to calculate the structural and residual portion energies, we only need the singular values of SVD decomposition. Hence, according to [7], we can obtain them with the order of $O(\min(mn^2, m^2n))$, where m and n are the number of image's rows and columns, respectively. To calculate the proposed metric, we need to call the SVD function twice and a loop with $O(q^2)$ iterations, and finally perform an averaging with $O(q)$. Thus the overall computational complexity of our metric summarized as $O(\min(mn^2, m^2n) + \min(m, n)^2)$. We compared our proposed metric with some other IQA indexes by running unoptimized MATLAB code (version R2013b) on a modern desktop with a 2.67GHz Intel Corei5 CPU and a 4G RAM. The average consuming times for assessing the blurriness of TID2008 images, with sizes of 512×384 , are shown in Table 3, ascendantly. It can be seen that the efficiency of our proposed metric is better than the most modern IQA indexes.

4 Conclusions

In this paper we addressed the image blurriness as two different distortions: destructed high frequency details, and redundancy-polluted low frequency structure. Motivated by this assumption, we proposed a novel full-reference blurriness measure, which extracts the two structural and nonstructural residual portions of the image. In the structural portion we assess the amount of low frequency redundancies, while in nonstructural residual portion we measure the amount of high-frequency degradation. These portions are constructed by summation of the SVD based basis image matrices corresponding to the low frequency and high frequency components of the image, respectively. We showed that the basis images corresponding to the higher singular values contain the structural information of the image, while the residual basis images provide the nonstructural details. The ratio of these portions energies for the reference and blurred images serves as the proposed blur metric.

The experimental results on images with various levels of blurriness convince the monotonic behavior of the proposed blurriness metric. In addition, the results achieved by applying the proposed metric on the blurred subsets of LIVE, TID2008 and CSIQ databases have also been quite satisfactory, showing a high correlation with the human perception of quality. The proposed metric has also been compared with other state-of-the-art blurriness metrics, standing among the best, specially have the first rank for the LIVE database.

References

1. Attar A, Shahbahrami A, Rad RM (2015) Image quality assessment using edge based features. *Multimedia Tools and Applications* pp 1–16, doi:[10.1007/s11042-015-2663-9](https://doi.org/10.1007/s11042-015-2663-9) (In press)
2. Batten CF (2000) Autofocusing and astigmatism correction in the scanning electron microscope. Mphil thesis, University of Cambridge
3. Cavedes J, Gurbuz S (2002) No-reference sharpness metric based on local edge kurtosis. In: *Proceedings of the IEEE international conference on image processing*, vol 3, pp III–53–III–56
4. Chung YC, Wang JM, Bailey RR, Chen SW, Chang SL (2004) A non-parametric blur measure based on edge analysis for image processing applications. In: *Conference on cybernetics and intelligent systems, 2004 IEEE*, vol 1, pp 356–360
5. Debing L, Zhibo C, Huadong M, Feng X, Xiaodong G (2009) No reference block based blur detection. In: *International workshop on quality of multimedia experience*, pp 75–80
6. Dijk J, Van Ginkel M, Van Asselt RJ, Van Vliet LJ, Verbeek PW (2003) A new sharpness measure based on gaussian lines and edges. In: *Computer Analysis of Images and Patterns*. Springer, pp 149–156
7. Golub GH, Van Loan CF (2012) *Matrix computations*, vol 3. JHU Press
8. Group VQE (2003) Final report from the video quality experts group on the validation of objective models of video quality assessment
9. Hassen R, Wang Z, Salama M (2010) No-reference image sharpness assessment based on local phase coherence measurement. In: *IEEE international conference on acoustics speech and signal processing (ICASSP)*, pp 2434–2437
10. Hassen R, Wang Z, Salama M (2013) Image sharpness assessment based on local phase coherence. *IEEE Transactions on Image Processing*
11. Kristan M, Per J, Pere M, Kovai S (2006) A bayes-spectral-entropy-based measure of camera focus using a discrete cosine transform. *Pattern Recogn Lett* 27(13):1431–1439
12. Larson EC, Chandler DM (2010) Most apparent distortion: full-reference image quality assessment and the role of strategy. *J Electron Imaging* 19(1):011, 006–011, 006–21
13. Li S, Zhang F, Ma L, Ngan KN (2011) Image quality assessment by separately evaluating detail losses and additive impairments. *IEEE Trans Multimedia* 13(5):935–949
14. Narwaria M, Lin W (2012) Svd-based quality metric for image and video using machine learning. *IEEE Trans Syst Man Cybern B Cybern* 42(2):347–364
15. Ponomarenko N, Lukin V, Zelensky A, Egiazarian K, Carli M, Battisti F (2009) Tid2008-a database for evaluation of full-reference visual quality assessment metrics. *Adv Mod Radioelectronics* 10(4):30–45
16. Sang Q, Qi H, Wu X, Li C, Bovik AC (2014) No-reference image blur index based on singular value curve. *J Vis Commun Image Represent* 25(7):1625–1630
17. Sheikh HR, Bovik AC (2006) Image information and visual quality. *IEEE Trans Image Process* 15(2):430–444
18. Sheikh HR, Wang Z, Cormack L, Bovik AC (2005) Live image quality assessment database release 2
19. Shnayderman A, Gusev A, Eskicioglu AM (2006) An svd-based grayscale image quality measure for local and global assessment. *IEEE Trans Image Process* 15(2):422–429
20. Su B, Lu S, Tan CL (2011) Blurred image region detection and classification. In: *Proceedings of the 19th ACM international conference on Multimedia, ACM*, pp 1397–1400
21. Tsomko E, Kim HJ (2008) Efficient method of detecting globally blurry or sharp images. In: *Ninth international workshop on image analysis for multimedia interactive services*, pp 171–174
22. Vu PV, Chandler DM (2012) A fast wavelet-based algorithm for global and local image sharpness estimation. *IEEE Signal Process Lett* 19(7):423–426
23. Wang S, Deng C, Lin W, Zhao B, Chen J (2013) A novel svd-based image quality assessment metric. In: *2013 20th IEEE International conference on image processing (ICIP)*
24. Wang S, Cui D, Wang B, Zhao B, Yang J (2014) A perceptual image quality assessment metric using singular value decomposition. *Circuits, Systems, and Signal Processing* 1–21, doi:[10.1007/s00034-014-9840-3](https://doi.org/10.1007/s00034-014-9840-3)
25. Wang Z, Bovik AC (2006) Modern image quality assessment. *Synth Lect on Image, Video, and Multimedia Process* 2(1):1–156
26. Wang Z, Simoncelli EP, Bovik AC (2003) Multiscale structural similarity for image quality assessment. In: *Proceedings of the 37th IEEE asilomar conference on signals, systems and computers*, vol 2, pp 1398–1402
27. Wang Z, Bovik AC, Sheikh HR, Simoncelli EP (2004) Image quality assessment: from error visibility to structural similarity. *IEEE Trans Image Process* 13(4):600–612
28. Wee CY, Paramesran R (2008) Image sharpness measure using eigenvalues. In: *9th IEEE international conference on signal processing*, pp 840–843

29. Zhang L, Zhang D, Mou X (2011) Fsim: a feature similarity index for image quality assessment. *IEEE Trans Image Process* 20(8):2378–2386
30. Zhu J, Wang N (2012) Image quality assessment by visual gradient similarity. *IEEE Trans Image Process* 21(3):919–933
31. Zhu X (2013) Qpro: An improved no-reference image content metric using locally adapted svd. In: *Proceedings of Seventh international workshop on video processing and quality metrics for consumer electronics*



Mohammad Hossein Khosravi received his B.Sc. degree in software engineering from the School of Electronic and Computer Engineering, Ferdowsi University of Mashhad, Mashhad, Iran, in 1996, and his M.Sc. degree from the Computer Engineering Department, Amirkabir University of Technology, Tehran, Iran, in 2004, majoring in artificial intelligence. He is currently pursuing the Ph.D. degree with the Laboratory of Image Processing and Data Mining, University of Shahrood, Shahrood, Iran. His research interest focuses on perceptual image quality assessment.



Hamid Hassanpour received the B.S. degree in computer engineering from Iran University of Science and Technology, Tehran, Iran, in 1993, the M.S. degree in computer engineering from Amirkabir University of Technology, Tehran, Iran, in 1996, and the Ph.D. from the Queensland University of Technology, Brisbane, Australia, in 2004. He has a professor position in faculty of Computer Engineering & IT at the University of Shahrood, Iran. His research interests include Image Processing, Signal Processing, timefrequency signal processing and analysis.